

## Electronic Supplementary Material for the Article

# Novel Design Approaches for Multifunctional Information Carriers

Melanie Ecker and Thorsten Pretsch\*

5

*BAM Federal Institute for Materials Research and Testing, Division 6.5, Polymers in Life Science and Nanotechnology, Unter den Eichen 87, 12205 Berlin, Germany. Email: thorsten.pretsch@bam.de*

## Table of contents

10	Experimental Section .....	SI
	Supporting Figures and Tables .....	SII
	Fig. S1 ATR-FTIR spectra .....	SII
	Fig. S2 Photographs of thermochromic PEU films .....	SII
	Fig. S3 Microscopic images of solvent cast PEU films .....	SII
15	Fig. S4 Scanning electron micrograph of a thermochromic PEU layer atop PEU substrate .....	SIII
	Fig. S5 DSC thermogram of a programmed type 1 QR code carrier .....	SIII
	Fig. S6 CIELAB values of a type 1 QR code carrier .....	SIV
	Fig. S7 Microscopic image of a type 2 QR code carrier .....	SIV
	Fig. S8 Michelson contrast of a type 2 QR code carrier .....	SV
20	Fig. S9 Thermochromic behavior of type 1 and type 2 QR code carriers after temperature cycling .....	SV
	Tab. S1 CIELAB values of a type 1 QR code carrier .....	SV

## Experimental Section

Attenuated Total Reflectance (ATR) Fourier Transform Infrared Spectroscopy (FTIR) measurements were performed with a Thermo  
25 Nicolet 6700 spectrometer using a DTGS detector. The ATR cell was equipped with a ZnSe crystal. The spectra were recorded from 4000 to 400 cm<sup>-1</sup> as the average of 32 scans at a resolution of 2 cm<sup>-1</sup>.

In order to determine layer thicknesses of solvent cast PEU films, cryomicrotome sections of the samples were prepared and  
microscopically investigated. The samples were prepared at -20 °C with a cryomicrotome CM1950 from Leica and were characterized  
30 by a thickness of 20 µm. The slices were studied with a Leica DM EP microscope at a 10 times optical zoom.

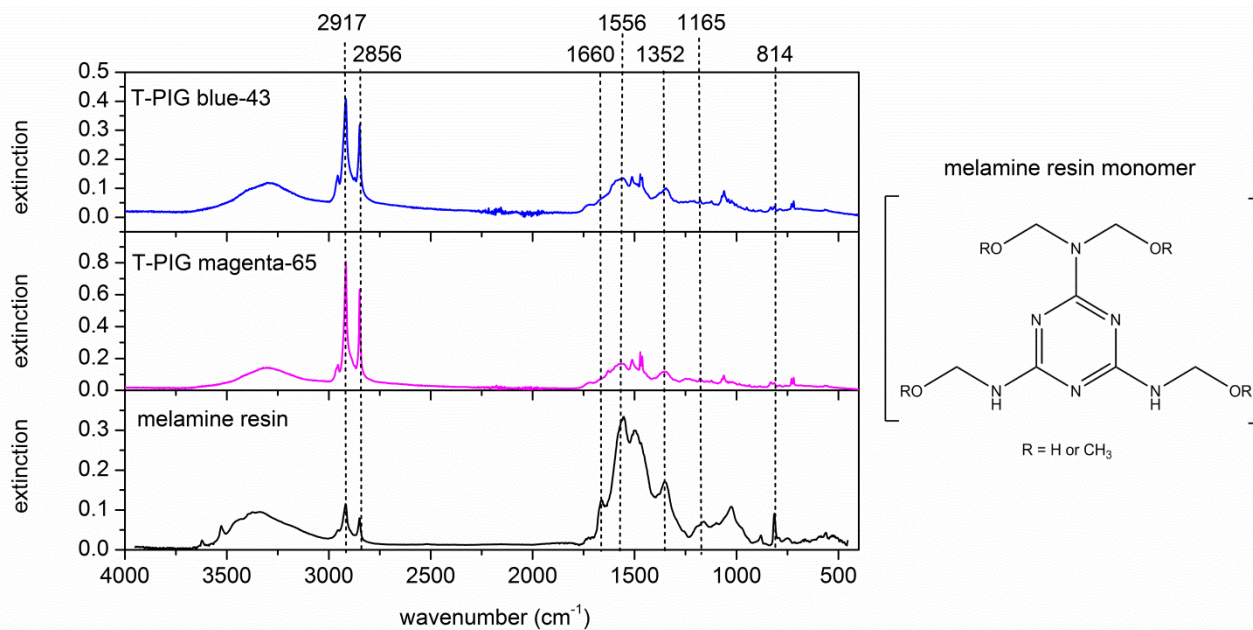
The CIE 1976 L\*a\*b\* (CIELAB) values were determined with the image editing program CorelDraw X6. Therefore, QR code carriers  
were temperature cycled between 20 and 70 °C and photographs were regularly taken. For all temperatures investigated, the values were  
determined as an average of three measurements at different subzones (at the position detection pattern) within the QR codes and the  
35 standard deviation was calculated. The temperature-dependent color difference ΔE was calculated from the CIELAB values as defined in  
Eq. 1 with reference to the values at 20 °C on heating and on cooling.

$$\Delta E = \sqrt{(L^* - L^*_0)^2 + (a^* - a^*_0)^2 + (b^* - b^*_0)^2} \quad (1)$$

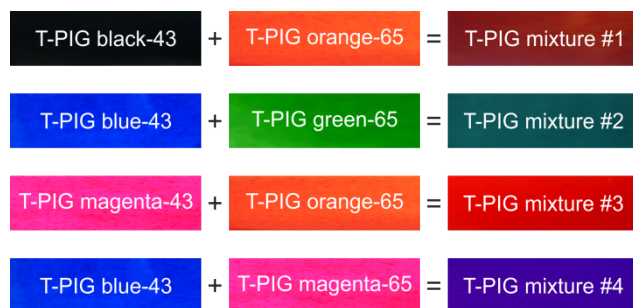
Scanning electron micrographs of cross-sections of type 1 QR code carriers were recorded with a Zeiss Gemini Supra 40 device, which  
40 operated at an extra high tension of 10 kV. The sample was coated with a few nanometers thin gold layer by means of a sputtering  
system.

A DSC measurement was conducted on a programmed type 1 QR code carrier whose PEU surface layer contained T-PIG mixture #4. For  
sample preparation, a piece of the information carrier weighing approximately 5 mg was cut. The sample was placed in an aluminum pan  
45 with the substrate pointing toward the bottom of the pan. The sample was cooled to -90 °C before it was heated to 90 °C with cooling  
and heating rates of 10 °C min<sup>-1</sup>.

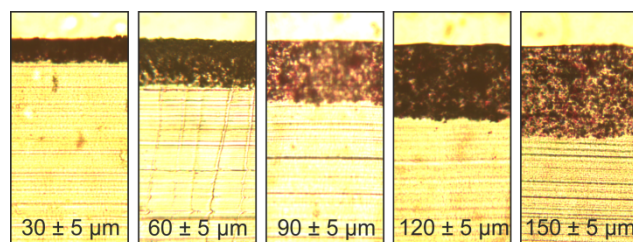
## Supporting Figures



5 **Fig. S1.** ATR-FTIR spectra of powdery T-PIG blue-43 and T-PIG magenta-65 and of melamine resin (reference data were taken from HR Thermo Nicolet Sample Library). The strong absorptions at 2917 and 2856 cm<sup>-1</sup> represent the asymmetric and symmetric stretching vibration  $\nu(\text{CH})$  of the methylene group of melamine resin. The peak at 1660 cm<sup>-1</sup> can be assigned to the  $\delta(\text{NH}_2)$ , the signals at 1556 and 1352 cm<sup>-1</sup> to the in-plane stretching vibration  $\nu(\text{C}=\text{N})$  of the 1, 3, 5-triazine ring, the band at 1165 cm<sup>-1</sup> to the deformation vibration  $\delta(\text{C}-\text{O})$  of the melamine resin and the signal at 814 cm<sup>-1</sup> to the out-of-plane deformation vibration of the triazine ring.



10 **Fig. S2.** Solvent cast PEU films containing 20 wt% of one sort of T-PIG with a CST of 43 °C (left column), 20 wt% of another sort of T-PIG with a CST of 65 °C (column in the middle) and 1:1 mixtures of both (right column). The films had uniform thicknesses of  $(65 \pm 5) \mu\text{m}$ . The images were recorded at 23 °C.



15 **Fig S3.** Microscopic images of solvent cast PEU films containing T-PIG mixture #4 atop PEU substrate. The thickness of the films could be controlled by means of a doctor blade.

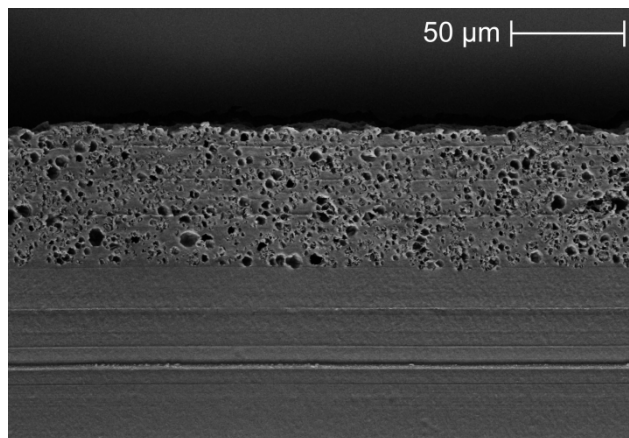
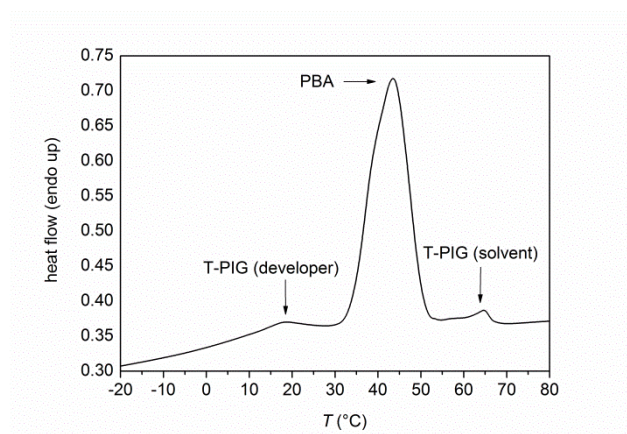


**Fig. S4.** Scanning electron micrograph of a PEU surface layer containing T-PIG mixture #4 atop PEU substrate.



**5 Fig. S5.** First DSC heating scan of a sample of programmed type 1 QR code carrier whose PEU surface layer contained T-PIG mixture #4. The PEU substrate was in direct contact with the aluminium pan.

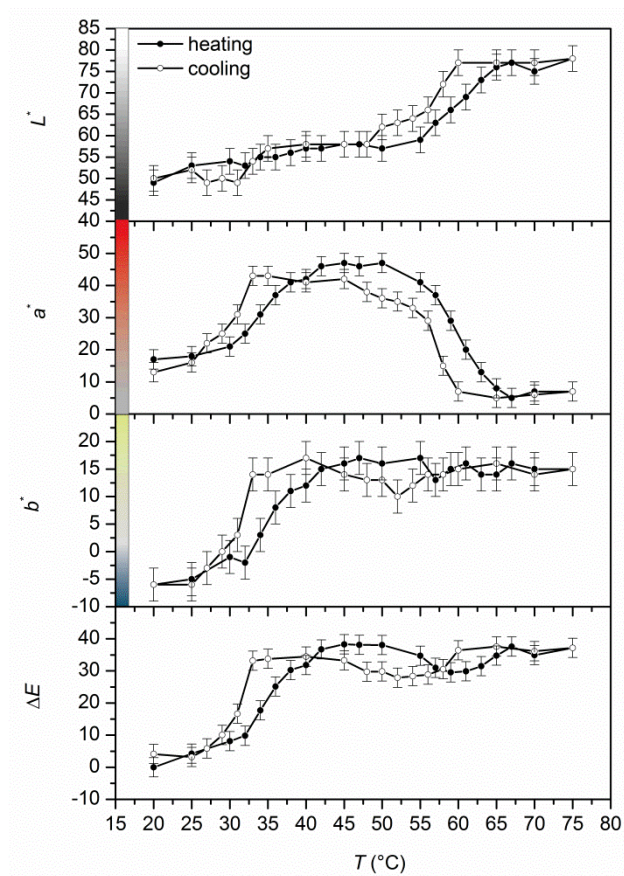
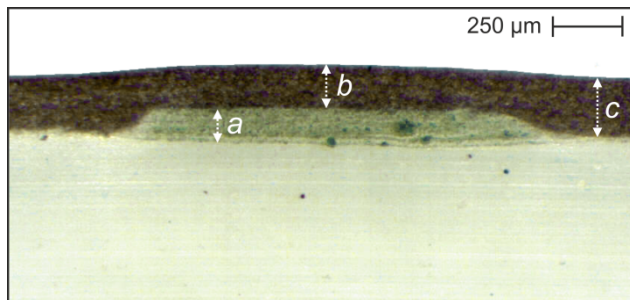
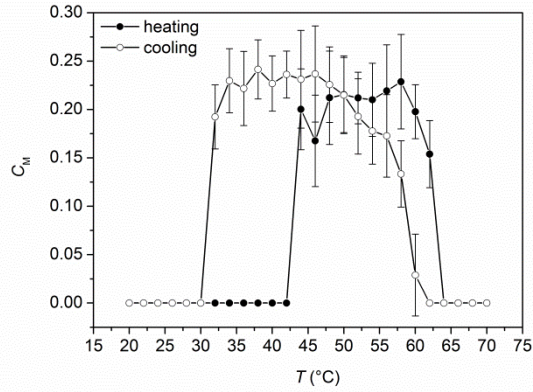


Fig. S6. Temperature-dependence of CIELAB values and color differences  $\Delta E$  of a type 1 QR code carrier whose PEU surface layer contained T-PIG mixture #4.



5

Fig. S7. Microscopic image of a type 2 QR code carrier containing T-PIG green-65 in a laser-engraved bottom layer and T-PIG black-43 in a continuous cover layer. Layer thicknesses of  $a = (119 \pm 6) \mu\text{m}$ ,  $b = (152 \pm 6) \mu\text{m}$  and  $c = (211 \pm 6) \mu\text{m}$  were determined.



**Fig. S8.** Temperature-dependent evolution of Michelson contrast  $C_M$  of a permanent-shaped type 2 QR code carrier containing T-PIG green-65 in a bottom layer and T-PIG black-43 in a cover layer.

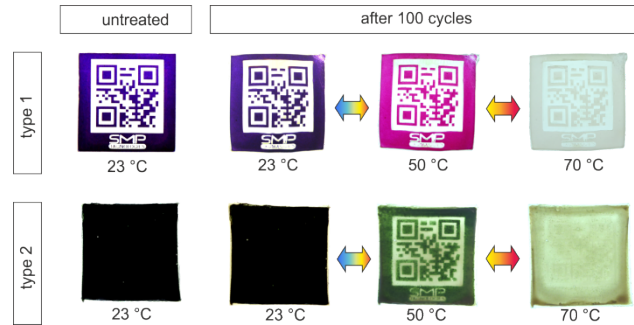


**Fig. S9.** Durability of thermochromic behavior in permanent-shaped type 1 and type 2 QR code carriers. The untreated states (left) are compared with the states at 23, 50 and 70 °C after running 100 heating-cooling cycles (right).

**Tab. S1.** CIELAB values and color differences  $\Delta E$  of a type 1 QR code carrier whose PEU surface layer contained T-PIG mixture #4. The values are provided for the untreated state and for the state after running 100 heating-cooling cycles between 23 and 70 °C.

sample	$T$ [°C]	$L^*$	$a^*$	$b^*$	$\Delta E$
untreated	23	$22.8 \pm 1.0$	$8.7 \pm 1.0$	$-7.7 \pm 1.0$	-
after 1 cycle	23	$24.2 \pm 1.0$	$8.4 \pm 1.0$	$-5.0 \pm 1.0$	$3.6 \pm 1.0$
after 100 cycles	23	$22.3 \pm 1.0$	$10.1 \pm 1.0$	$-8.3 \pm 1.0$	$2.1 \pm 0.8$
untreated	50	$26.4 \pm 1.0$	$26.4 \pm 1.0$	$-1.0 \pm 1.0$	-
after 1 cycle	50	$29.9 \pm 1.0$	$25.4 \pm 1.0$	$1.1 \pm 1.0$	$4.8 \pm 1.0$
after 100 cycles	50	$27.8 \pm 1.0$	$28.8 \pm 1.0$	$-0.2 \pm 1.0$	$3.2 \pm 1.7$